

Threshold Photoneutron Cross Section for $\text{Fe}^{56}\dagger$

C. D. BOWMAN, G. S. SIDHU, AND B. L. BERMAN

Lawrence Radiation Laboratory, University of California, Livermore, California

(Received 5 June 1967)

Individual levels of the compound nucleus Fe^{56} at an excitation energy of 11.2 MeV have been studied by examining the (γ, n) cross section for natural iron from 0.7 to 70 keV above threshold with high resolution. The technique is generally applicable to the high-resolution study of photoneutron cross sections for photons whose energy exceeds the photoneutron threshold by an amount of the order of the order of keV. Resonance parameters were obtained for certain favorable cases. The γ -ray strength function $\langle \Gamma_{\gamma_0}/D \rangle$ for electric dipole absorption in Fe^{56} was found to be 3.5×10^{-6} , which is a factor of 2 lower than the estimates obtained either from the low-energy wing of the giant dipole resonance or from the single-particle model of the nucleus.

I. INTRODUCTION

THIS paper reports the results of a neutron time-of-flight measurement of the photoneutron cross section within a few tens of kilovolts of threshold performed with good resolution. Such measurements allow one to explore in detail the properties of many individual nuclear levels just above the neutron separation energy in all stable nuclei, and thus to investigate several classes of systematics of the excited nucleus. Also, the multipolarity and strength of the electromagnetic transitions which excite the nuclear states can be determined when the technique is applied properly.

In this experiment, bursts of electrons from the Livermore electron linear accelerator are used to produce bremsstrahlung which, in turn, irradiates the (γ, n) sample under study. In this way, narrow resonances of the compound nucleus can be excited by photon absorption. The energy of the electrons is adjusted so that the tip of the bremsstrahlung spectrum barely exceeds the neutron-binding energy [or the (γ, n) threshold] for the sample. Therefore, neutron transitions from the levels of the compound nucleus to excited states of the residual nucleus (target minus one neutron) cannot take place, and only ground-state transitions are energetically possible. The neutron energy thus is equal to the γ -ray energy minus the neutron-binding energy. The neutron energy can be determined and individual states resolved by the rather well-developed time-of-flight technique of slow- and intermediate-energy neutron spectroscopy. The idea is not entirely a new one, and there has been an attempt to exploit it before;¹ the new departure introduced here is to look for resonances in the neutron-energy spectrum in the very low-energy region from zero to a few tens of kilovolts with a highly efficient slow-neutron detector. This method, as applied here, is capable of neutron-energy resolution of a few tens of eV for incident photon energies of 10 MeV. The resolution can be improved to the limit imposed by the thermal motion of the target nuclei, provided that

sufficiently intense and short bursts of bremsstrahlung are available.

Consider the case of the reaction $\text{Fe}^{56}(\gamma, n)\text{Fe}^{55}$ (see Fig. 1). If Fe^{56} is irradiated with bremsstrahlung having a maximum energy between 11.21 and 11.62 MeV, all the resonances seen in the neutron energy spectrum can be identified unambiguously as representing levels in Fe^{56} having excitation energy equal to the neutron-binding energy plus the resonance energy (corrected for the photon and neutron momenta and the recoil of the residual Fe^{55} nucleus). Thus, one can examine in great detail the band of levels from zero to about 70 keV above the (γ, n) threshold in Fe^{56} ; the upper limit is set by the intense scattered photons which desensitize the detector for a few microseconds following the bremsstrahlung burst. The incident γ -ray intensity is nearly the same for all resonances in this energy interval, since the photon energy changes only by 0.6% over this range.

For many target nuclei these experiments can determine the spin, parity, neutron width, and ground-state γ -ray transition width for many excited states of

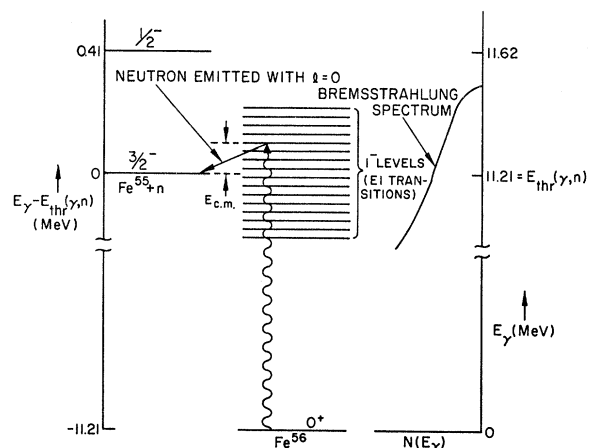


FIG. 1. Schematic representation of the experiment. The figure shows a schematic representation of the predominant interaction mechanism, s -wave neutron emission following electric dipole photon absorption. The energy-level spectrum for Fe^{56} is shown in the center of the figure. The spectrum for Fe^{55} is displaced by the neutron binding energy. The endpoint of the bremsstrahlung photon spectrum which induces the reaction is shown in relation to the level spectra of the target and residual nuclei.

[†] This work was performed under the auspices of the U. S. Atomic Energy Commission.

¹ W. Bertozzi, C. P. Sargent, and W. Turchinets, *Phys. Letters* **6**, 108 (1963).

the target nucleus. This information is obtained for a set of compound nuclei which generally cannot be studied by neutron cross-section measurements. In addition to such information on individual levels, these experiments can provide a wealth of statistical information on nuclear level densities for levels of a particular value of spin and parity, γ -ray strength functions for electromagnetic transitions of specified multipolarity, and neutron strength functions for specified neutron angular momentum.

II. EXPERIMENT

The experiment consisted of measuring the time-of-flight spectrum of the low-energy photoneutrons from iron. The experimental arrangement is shown in Fig. 2. The electron beam from the linear accelerator was collimated and energy-analyzed with a bending magnet and graphite slit arrangement, and then allowed to strike a 2.58-cm-thick Al bremsstrahlung-producing target. The target was thick enough to stop completely the primary electron beam. This insulated target then was used as a crude beam monitor as well. The bremsstrahlung photons in turn irradiated a 1.25-cm-thick iron sample which was placed along the line of sight of the neutron detector. The angle between the neutron flight path and the bent electron beam (and hence the photon beam) was 135° . The 7.62-cm-diam sample was placed at an angle of 67.5° with respect to each of the above (see Fig. 2). The neutron detector consisted of a B^{10} -loaded liquid scintillator, 12.75 cm in diameter by 1.60 cm thick, which was viewed by a 12.75-cm EMI 9579B phototube. The signals were amplified, shaped, and then fed into a 4096-channel TMC time analyzer. The effect of the γ flash from the electron beam burst was reduced by pulsing the second dynode of the photomultiplier tube positive during the γ flash. In this way the tube was gated off until the burst of scintillator light had decayed to a sufficiently low level for neutron detection. The detector was located 18.6 m from the

iron sample. A 3-ft-deep hole in the shield wall behind the sample (see Fig. 2) prevented neutrons from the wall from reaching the detector directly. A 1.5-m-thick concrete shield wall between the detector and the target room is not shown on the drawing.

Two measurements were made to obtain the results presented in this paper. Earlier work² had indicated that the major features of the cross section are associated with neutron transitions to the ground state of Fe^{55} , even though neutron emission to the first and second excited states was energetically possible. In that experiment, the electron energy was 12.5 MeV, which exceeded the energy required for neutron emission to the second excited state. This choice of energy was made to increase the photon intensity at the energies corresponding to kilovolt neutron emission to the ground state of Fe^{55} , at the risk of some confusion in the interpretation of the resulting data. The first of the present measurements was carried out with an electron beam of energy 12.7 MeV, a pulse repetition rate of 360 pps, a pulse width of 120 nsec, and a current during the pulse of 0.18 A. The spread of the energy of the electron beam was such that half the electrons which struck the bremsstrahlung target had an energy within 120 keV of the central energy of 12.7 MeV, and all were within 450 keV of it. The object of the more recent measurement was to obtain improved counting statistics and resolution over that of the earlier experiment. A second, shorter measurement was made under the same conditions except with an electron energy of 11.6 MeV. Since neutrons could, in this measurement, be emitted only to the ground state of Fe^{55} , such a measurement, which reproduced the salient features of the measurement at higher electron energy, was adequate to show that these features were associated with ground-state transitions.

III. THE NEUTRON DETECTOR

For these measurements, the calculated cross section is inversely proportional to the neutron detector efficiency; and since the neutron energy varies from 800 eV to 70 keV, it is important to know the energy dependence of this efficiency in order to obtain accurate cross-section data. In addition, the time response of the detector is large compared to the other time uncertainties, so that the energy resolution in this experiment is determined largely by the detector response. The details of construction of the detector are given elsewhere.³

The detector efficiency was measured by using the linear accelerator as a pulsed source of neutrons. The neutron detector rate in the scintillator was compared with that of a B^{10} proportional counter. The unnormalized efficiency was obtained assuming a cross section inversely proportional to the neutron velocity for the

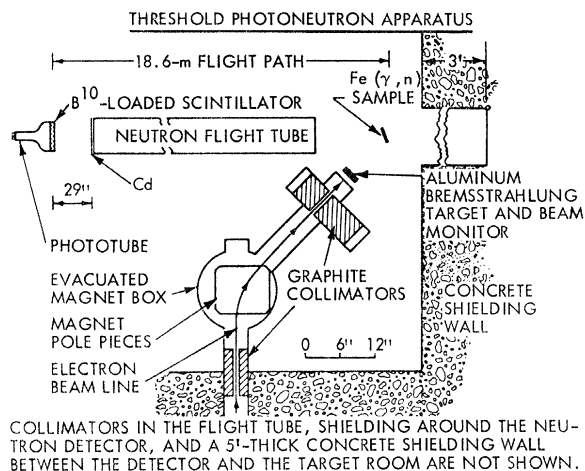


FIG. 2. Experimental apparatus.

² B. L. Berman, G. S. Sidhu, and C. D. Bowman, *Phys. Rev. Letters* **17**, 761 (1966).

³ G. D. Sauter, Ph.D. thesis, University of California, 1966 (unpublished).

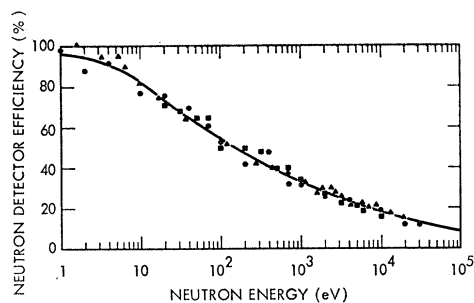


FIG. 3. The neutron detector efficiency.

B^{10} . The results of a Monte Carlo calculation of the detector efficiency for 1.5-eV neutrons was used to normalize the efficiency curve. The resulting efficiency plotted as a function of neutron energy is shown in Fig. 3. The triangular, rectangular, and circular points distinguish the results of three independent measurements. The line drawn through the data was used in the conversion of the time spectrum to cross section. The Monte Carlo code also was used to calculate the efficiency as a function of energy. Unfortunately, the code could not easily be arranged to include the effects of backscattering from the glass and other components of the photomultiplier tube. Excellent agreement between the calculated and measured efficiency was obtained at energies below about 500 eV. However, above this energy the neglect of backscattering causes the calculated efficiency to fall below the measured efficiency. The discrepancy increases with energy and at 40 keV reaches 25%.

Although the calculation did not give data on the efficiency in the kilovolt region with sufficient accuracy to be useful, it did yield, along with other information, the probability $P(t)$ for detecting a neutron at a given time t after entering the detector. The mean capture time \bar{t} therefore can be obtained from the relation

$$\bar{t} = \frac{\int_0^{\infty} tP(t)dt}{\int_0^{\infty} P(t)dt} = \frac{1}{\epsilon} \int_0^{\infty} tP(t)dt, \quad (1)$$

where ϵ is the detector efficiency. Since $P(t)$ occurs in both the numerator and the denominator of this expression, the absolute error in determining the efficiency does not limit, to a serious degree, the calculation of meaningful values of \bar{t} . The quantity \bar{t} plotted as a function of neutron energy is shown in Fig. 4.

The time resolution of the neutron detection system is determined primarily by four factors: the uncertainty in the flight path (2 cm), the width of the electron burst (0.12 μ sec), the time-analyzer channel width (0.0625 μ sec), and the mean capture time in the scintillator. It is clear from Fig. 4 that over most of the energy range of this experiment the experimental resolution is determined primarily by the detector response. The nominal time resolution for these experiments was 15 nsec/m.

IV. DATA REDUCTION TO CROSS SECTION

The data first were corrected for the background which was not correlated in time with the beam burst. This background was measured continuously throughout the experiment with the time analyzer by extending the range of the analyzer to a time well beyond that corresponding to the cutoff neutron energy for a cadmium filter placed in the flight tube. The average number of background events per time channel obtained from the time channels beyond this cutoff was subtracted from all the time channels corresponding to energies in excess of 500 eV. This is the only background correction which was applied to the data.

The absolute laboratory photoneutron cross section σ_{lab} (4π times the differential cross section) as a function of the neutron energy E_L was then calculated according to the formula

$$\sigma_{\text{lab}}(E_L) = KC(E_L)/\epsilon(E_L), \quad (2)$$

where $C(E_L)$ is the number of detected events per unit neutron energy interval, $\epsilon(E_L)$ is the neutron detector efficiency, and K is a constant which is very nearly independent of the neutron energy and depends only on the fixed parameters of the system for a given measurement. In terms of the number of counts per channel $C(i)$, this becomes

$$\sigma_{\text{lab}}(E_L) = 672KC(i)[\epsilon(E_L)WE_L^{3/2}]^{-1}, \quad (3)$$

where W is the channel width in μ sec/channel, E_L is in eV, and the path length is 18.6 m. The parameter K includes or accounts for the total number of electrons incident on the bremsstrahlung target during the experimental run, the bremsstrahlung conversion efficiency, the solid angles subtended by the neutron sample at the bremsstrahlung target and by the neutron detector at the neutron sample, the sample thickness, the isotopic abundance, the attenuation of the photon beam in the sample and of the neutron beam in passing through the various materials in the flight path (e.g., windows, air gaps, cadmium, etc.), and the efficiency of the detection and counting apparatus for recording a true event. The thick-target bremsstrahlung yield was calculated with the aid of a computer code based on the

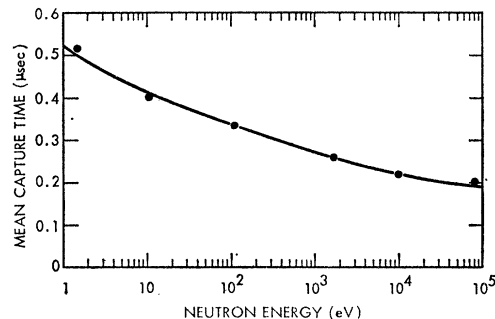


FIG. 4. Mean capture time for the neutron detector.

Schiff differential formula,⁴ and includes the effects of self-absorption and multiple electron scattering in the bremsstrahlung converter by means of a Gaussian approximation to the Molière distribution.⁵ This multiple-Coulomb scattering also was taken into account in the photon solid-angle calculation.

For some purposes, such as for fitting Breit-Wigner formulas, it is convenient to transform the cross section into the center-of-mass system. The relationship required is

$$\sigma_{c.m.}(E) = \sigma_{lab}(E_L) [d\Omega_L(E_L)/d\Omega_{c.m.}(E_{c.m.})], \quad (4)$$

where $\sigma_{c.m.}$, E , $E_{c.m.}$ and $d\Omega_{c.m.}$ are the cross section, the total energy, the neutron energy, and the differential solid angle in the center-of-mass system, respectively, and $d\Omega_L$ is the differential solid angle in the laboratory system. The derivative in Eq. (4) can be obtained from the expression

$$\cot\theta_{c.m.} = \cot\theta_L - \left[\frac{M-m}{m} \right] \frac{2Mc^2/E_\gamma}{\left[1 - (Q/E_\gamma) - (E_\gamma/2Mc^2) \right]^{1/2}} \csc\theta_{c.m.}, \quad (5)$$

where E_γ is the photon energy, m and M are the masses of the neutron and target nucleus, respectively, Q is the neutron binding energy, c is the velocity of light, and $\theta_{c.m.}$ and θ_L are the neutron angles in the center-of-mass and laboratory systems, respectively. Since $d\Omega_L/d\Omega_{c.m.} = d(\cos\theta_L)/d(\cos\theta_{c.m.})$, the derivative of Eq. (5) can be used in Eq. (4) to obtain

$$\sigma_{c.m.}(E) = \sigma_{lab}(E_L) (1 - \alpha \cos\theta_L) (1 - 2\alpha \cos\theta_L + \alpha^2)^{1/2}, \quad (6)$$

where

$$\alpha^2 = (m/M) (E_\gamma/2Mc^2) (E_\gamma/E_L).$$

The relationship between the laboratory neutron energy E_L and the total energy in the center-of-mass system E is

$$E = Q + \left[\frac{M}{M-m} \right] [1 - 2\alpha \cos\theta_L + \alpha^2] E_L. \quad (7)$$

It also might be useful to compare the (γ, n) cross section with the inverse cross section, (n, γ) , when the correlation between the two experiments can provide additional information. The neutron energy E_n required in the (n, γ) experiment in order to obtain the same excitation energy in the center-of-mass system as the (γ, n) experiment is related to E by the expression

$$E_n = \left[\frac{M}{M-m} \right] [E - Q]. \quad (8)$$

V. RESULTS

A. Cross Section

The laboratory cross section σ_{lab} measured at 135° is plotted against the observed neutron energy in Figs. 5 and 6. The absolute cross-section scale is uncertain by $\pm 30\%$, owing to the uncertainty in the fraction of the bremsstrahlung radiation intercepted by the iron

⁴ L. I. Schiff, Phys. Rev. **83**, 252 (1951).

⁵ G. Molière, Z. Naturforsch **3a**, 78 (1948).

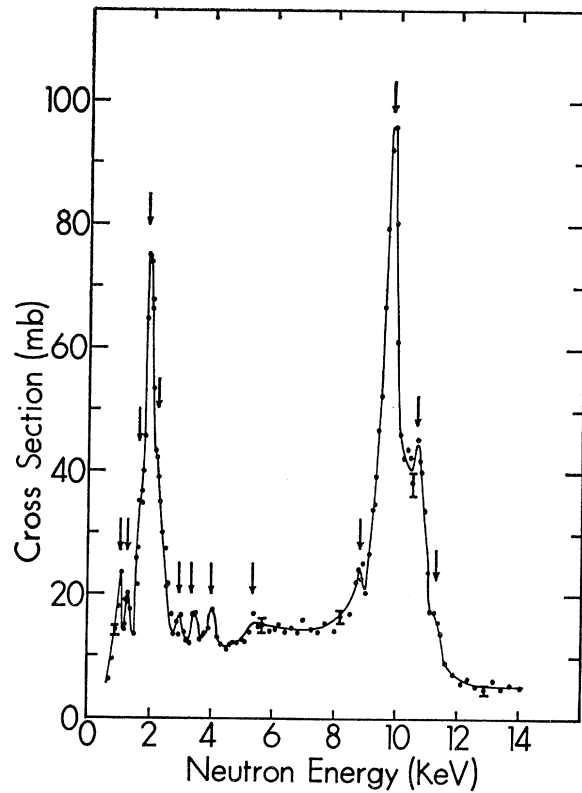


Fig. 5. Absolute photoneutron cross section $\sigma = 4\pi (d\sigma/d\Omega)_{135^\circ}$. The counting statistics for this experiment are shown for a few points by the error bars. The absolute cross-section scale is uncertain to $\pm 30\%$. The energies of the peaks denoted by the vertical arrows are tabulated in Table I.

sample. The energies at which the resonances were observed (at 135° to the photon direction) are listed in Table I, along with $(E-Q)$, which is the total kinetic energy in the center-of-mass system after the neutron has been ejected from the target nucleus by the photon, and with E_n , the energy of the neutron required to excite the same resonance in a neutron capture reaction. These calculations were carried out using Eqs. (7) and (8) for a photon energy of 11.2 MeV.

The two large peaks in Fig. 5 were observed in earlier work on this nucleus,² but are seen here with much better energy resolution and statistics. Measurements with a peak electron energy of 11.6 MeV showed conclusively that these two peaks belong to the Fe^{56} compound nucleus. It cannot be said with certainty that the smaller peaks also are associated with the Fe^{56} compound nucleus. These peaks cannot be attributed to neutron emission from the isotope Fe^{54} since its photoneutron threshold of 13.6 MeV is well above the bremsstrahlung endpoint energy. In the measurements reported here, neutron emission from Fe^{58} is energetically possible, since its photoneutron threshold occurs at 10.05 MeV. However, since this isotope is only 0.33% abundant, its contribution to the measured cross section probably is not important. However, Fe^{57}

cannot be eliminated as a contributor to the measured cross section, even though its isotopic abundance is only 2.19%. Since its photoneutron threshold is 7.64 MeV, the effective bremsstrahlung intensity is higher for this nucleus than for Fe⁵⁶. The bremsstrahlung intensity for 12.6-MeV electrons is five times as large at 7.64 MeV as at 11.2 MeV, and the Fe⁵⁷ fraction therefore is equivalent to a 10% contamination in the spectrum.

Those resonances which correspond to neutron emission from Fe⁵⁷ to the ground state of Fe⁵⁶ also should be seen in the inverse reaction; namely, the neutron capture cross section of Fe⁵⁶. Of course, all the peaks seen in such a measurement would not necessarily be seen here since only those resonances which have a strong ground-state γ -ray transition strength are observable. However, there appears to be no obvious correspondence between the structure observed here and that observed in the inverse reaction.⁶⁻⁸ This might result from the 0.25- μ sec uncertainty in the time calibration for this experiment. The determination of the magnitude of the contribution from Fe⁵⁷ to the

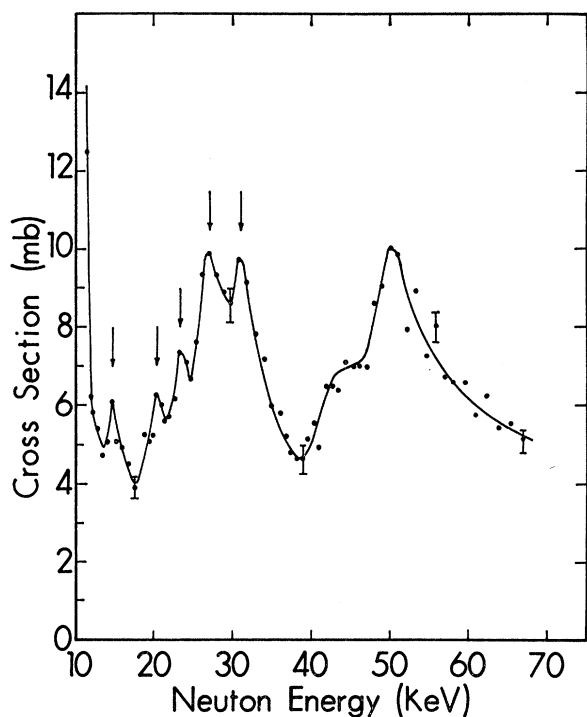


FIG. 6. Absolute photoneutron cross section $\sigma = 4\pi(d\sigma/d\Omega)_{135^\circ}$. The counting statistics for this experiment are shown for a few points by the error bars. The absolute cross-section scale is uncertain to $\pm 30\%$. The energies of the peaks denoted by the vertical arrows are tabulated in Table I.

⁶ M. C. Moxon, in *Proceedings of the International Conference on the Study of Nuclear Structure with Neutrons, Antwerp* (North-Holland Publishing Company, Amsterdam, 1965), Paper 88.

⁷ R. L. Macklin, P. J. Pasma, and J. H. Gibbons, *Phys. Rev.* **136**, B695 (1964).

⁸ J. A. Moore, H. Palevsky, and R. E. Chrien, *Phys. Rev.* **132**, 801 (1963).

TABLE I. Energies of peaks in the cross section.

E_L^a (keV)	$(E-Q)^b$ (keV)	E_n^c (keV)
1.05	1.28	1.30
1.25	1.51	1.54
1.65	1.94	1.97
1.92	2.22	2.26
2.20	2.54	2.58
2.95	3.36	3.42
3.40	3.84	3.91
4.00	4.49	4.57
5.35	5.92	2.06
8.80	9.55	9.71
9.80	10.62	10.8
10.65	11.50	11.7
11.30	12.2	12.4
14.70	15.9	16.2
21.0	22.3	22.7
23.5	24.9	25.4
27.0	28.5	29.0
31.0	32.6	33.2

^a E_L is the energy of the neutrons at the peaks in the cross section measured at 135° in the laboratory system. The uncertainty in flight time, which was 0.25 μ sec, corresponds to an uncertainty in energy (not shown in the table) of ± 0.01 keV at $E_L = 1$ keV and ± 2 keV at 31 keV.

^b $E-Q$ is the total kinetic energy in the center-of-mass system after photoejection of the neutron from the target nucleus. All resonances were assumed to belong to the Fe⁵⁶ compound nucleus.

^c E_n is the neutron energy required to excite the same resonance by the Fe⁵⁶(n, γ) reaction.

present measured cross section must await photoneutron measurements on a separated isotopic sample of Fe⁵⁷. The difference between $(E-Q)$ and E_L is about 20% less than that shown in Table I, if it is assumed that the neutrons are emitted from Fe⁵⁷.

B. Resonance Parameters and Strength Functions

Resonance parameters have been derived only for the 1.92- and 9.80-keV resonances. Area analysis of these two resonances was not attempted, since it is clear that for both peaks there are many resonances in the wings which could introduce large uncertainties in the resonance parameters obtained in that way. However, it does appear that shape analysis can be used to obtain both the neutron and the γ -ray widths for these resonances.

Shape analysis is based on the formula⁹

$$\sigma_{\gamma n} = \pi \lambda^2 g \Gamma_{\gamma 0} \Gamma_n / (E - E_0)^2 + \frac{1}{4} \Gamma^2, \quad (9)$$

where λ is the wavelength of the photon divided by 2π and g is a statistical factor equal to $(2J+1)/2(2I+1)$, where J and I are the spins of the compound nucleus state and target ground state, respectively. The parameter $\Gamma_{\gamma 0}$ is the width for decay of the compound state by γ -ray emission, Γ_n is the width for decay of the compound nucleus by neutron emission, and $\Gamma = \Gamma_n + \Gamma_{\gamma 0} + \sum_i \Gamma_{\gamma i}$, where $\Gamma_{\gamma i}$ is the width for γ -ray decay of the compound nucleus to any state i other than the ground state. The parameter E_0 is the energy of the resonance. Since the total γ -ray width $\Gamma_{\gamma} = \Gamma_{\gamma 0} + \sum_i \Gamma_{\gamma i}$ does not exceed a few eV for nearby nuclei,⁷ the total width is equal to the neutron width to a good approximation.

⁹ H. A. Bethe and G. Placzek, *Phys. Rev.* **51**, 150 (1937).

TABLE II. Parameters from shape analysis.

E_n (eV)	Resolution (eV)	FWHM ^a (eV)	σ_{obs} (mb)	σ_0 (mb)	$\Gamma \cong \Gamma_n$ (eV)	$g\Gamma_{\gamma 0}^b$ (eV)
1920	66±22	420	73	75	415	0.80
9800	340±120	660	96	136	560 ₊₅₀ ⁻¹⁰⁰	1.93 _{-0.15} ^{+0.1}

^a Full width at half maximum.

^b These numbers do not include the 30% uncertainty in the normalization of the cross section.

Therefore, one can obtain values for $\Gamma_{\gamma 0}$ and Γ_n from this analysis. The peak height, with these approximations, is given by $4\pi\lambda^2 g\Gamma_{\gamma 0}/\Gamma_n$, and the full width at half-maximum is $\Gamma \cong \Gamma_n$. When the resonances are resolved rather well, one can use these two quantities to find values for the parameters $g\Gamma_{\gamma 0}$ and Γ_n .

The pertinent parameters used in this analysis and the results are given in Table II. The first column contains the neutron energy in eV; the second column the full width at half-maximum of the energy resolution; the third column the full width at half-maximum of the observed width of the peak; the fourth column the maximum observed cross section σ_{obs} ; the fifth column contains the maximum cross section unbroadened by the resolution; the sixth column contains the neutron width Γ_n derived from the data; and the seventh column the value for $g\Gamma_{\gamma 0}$ obtained from the analysis of the width and peak heights. For both resonances the resolution function was assumed to be Gaussian in shape, and on this basis the width of the resonance was obtained by subtracting the measured full width at half-maximum and the resolution in quadrature. The total width thus obtained, together with the resolution, then was used to determine the reduction in peak height from the true peak height owing to the particular ratio of the resolution width to the resonance width. This was done with the aid of tables¹⁰ used for calculating line shapes which assume a Gaussian shape for the resolution function and a Breit-Wigner shape for the resonance.

The full width at half-maximum was determined for the 1.92-keV resonance by first plotting the highest seven points. The curve through these points was extrapolated down to 37 mb, and the measured width of the peak at this cross section value was used to obtain Γ . The resonance is resolved almost completely, since the total width is about six times the resolution function width. The full width at half-maximum for the peak at 9.80 keV was measured directly from the cross-section plot at an ordinate of 48 mb. The measured peak height was reduced significantly from the true peak height in this case, since the measured width is only about twice the width of the resolution function.

The errors on Γ_n and $g\Gamma_{\gamma 0}$ were obtained from a

consideration of the effects of a 30% uncertainty in the neutron energy resolution. The 30% uncertainty in the absolute normalization of the cross section does not add to the uncertainty in Γ_n , but imposes an additional 30% uncertainty on the value for $g\Gamma_{\gamma 0}$.

The spin of the resonances can be assigned by consideration of the spins of the target and residual nuclei and the orbital angular momentum of the neutron. The neutron widths for the resonances are within a factor of 2 of the Wigner limit¹¹ for $l > 0$; thus, the resonances are almost certainly de-excited by s -wave neutron emission. Since J^π for the ground state of Fe⁵⁵ is $\frac{3}{2}^-$, the spins of the resonances are restricted to the values 1^- or 2^- . The multipolarity of the electromagnetic transition from the 0^+ ground state of the Fe⁵⁶ target nucleus therefore must be either electric dipole or magnetic quadrupole. Since the $E1$ transition is estimated to be about 10^4 times stronger than the $M2$ transition,^{12,13} the spin assignment of 1^- for these states is almost surely correct. Thus, the value of g is $\frac{3}{2}$ for both resonances, and the values for $\Gamma_{\gamma 0}$ are $\frac{2}{3}$ of the values for $g\Gamma_{\gamma 0}$ listed in the table.

The possibility of associating the small resonances with neutron emission from Fe⁵⁷ has been discussed above. However, these resonances also could be weak resonances associated with p -wave neutron emission from Fe⁵⁶. It is useful to consider the influence of a neutron angular momentum greater than zero on the area under a resonance. The area under a Breit-Wigner resonance is given by the expression

$$A = 2\pi^2\lambda^2 g\Gamma_{\gamma 0}\Gamma_n/\Gamma. \quad (10)$$

For the two resonances analyzed thus far, the neutron width is more than 100 times the γ -ray width, and in this approximation the area under the resonance is proportional simply to $g\Gamma_{\gamma 0}$, since $\Gamma_n \cong \Gamma$. If the neutron width were much smaller, and about equal to the γ -ray width, then, for the same value of the γ -ray width, the area under the resonance would be reduced only by a factor of about 2. The ratio of the barrier penetration factor for p -wave neutrons to that for s -wave neutrons at 6 keV is 10^{-2} . Thus, if for this nucleus the $M1$ and $E1$ strengths are roughly equal just above the photon-neutron threshold, the area under the resonances excited by $M1$ absorption would be equal to that for those excited by $E1$ absorption, even though the widths for s -wave and p -wave neutron emission differed by a factor of 100. At this point, no more definite statement can be made regarding the character of these small resonances.

These data also can be analyzed for the electric dipole γ -ray strength function $\langle \Gamma_{\gamma 0}/D \rangle$ (D is the level spacing), which can be predicted from nuclear theory. A value can be obtained with the two resonances at 1.90 and 9.80 keV by averaging their values of $\Gamma_{\gamma 0}$ and

¹⁰ M. E. Rose, W. Miranker, P. Leak, L. Rosenthal, and J. K. Hendrickson, AEC Report No. WAPD-SR-506 (Vol. 1 and 2), Technical Information Extension, Oak Ridge, Tennessee (unpublished).

¹¹ T. Teichman and E. P. Wigner, Phys. Rev. **87**, 123 (1952).

¹² S. A. Moszkowski, Phys. Rev. **83**, 1071 (1951); **89**, 474 (1953).

¹³ V. F. Weisskopf, Phys. Rev. **83**, 1073 (1951).

dividing by the spacing between. However, the statistical sample is very poor, so that the value obtained in this way (13×10^{-5}) probably is not representative of the average strength for photon interactions. A more meaningful value can be obtained from the average cross section over the full-range measurement from 0.8 to 67.5 keV. The relation between this integral and the strength function can be written as

$$\bar{\sigma}(E) = \int_{\Delta E} \sigma dE / \Delta E = n\bar{A}/\Delta E \\ = 2\pi^2\chi^2g \left\langle \frac{\Gamma_{\gamma 0}}{D} \right\rangle \left\langle \frac{\Gamma_n}{\Gamma} \right\rangle, \quad (11)$$

where $\bar{\sigma}(E)$ is the average cross section, n is the number of resonances in the energy interval ΔE , \bar{A} is the average area under such a resonance, where use has been made of Eq. (10). The value for $\langle \Gamma_{\gamma 0}/D \rangle$ obtained in this way is 3.5×10^{-5} . The 30% uncertainty in the absolute cross section implies the same uncertainty in this quantity as well. The contributions from Fe^{57} , when subtracted from the data, might reduce this value by 10%. Some of the cross section could be attributed to p -wave neutron emission, which implies photon absorption other than by electric dipole; this also tends to reduce this value. Since these uncertainties are not resolved, the value of the electric dipole strength function thus obtained is an upper limit. Although values for the neutron width for two resonances have been measured, it is not meaningful to attempt to obtain values for the neutron strength function or the level spacing separately, since it is clear that there are many levels of unknown spin which could influence these two quantities in an unknown way. Therefore, no values for these quantities are given here.

This value for the γ -ray strength function can be compared with estimates obtained from an extrapolation of the lower-energy wing of the giant dipole resonance,¹⁴ and with predictions of the single-particle model.^{12,13} The value of the cross section predicted from the wing of the giant dipole resonance can be determined to sufficient accuracy by averaging the values of the wings of the Lorentz fits to the giant resonances for V and Co,¹⁵ and is found to be 5.5 mb at 11.2 MeV. Under the assumptions that the cross section results from electric-dipole transitions only and that $\Gamma_n \simeq \Gamma$, Eq. (11) then yields a value for $\langle \Gamma_{\gamma 0}/D \rangle$ of 6×10^{-5} . The prediction of the single-particle shell model for the dependence of $\langle \Gamma_{\gamma 0}/D \rangle$ on the atomic weight A and on E_γ has been written by Axel¹⁴ in the form

$$\langle \Gamma_{\gamma 0}/D \rangle = C(E_\gamma/7 \text{ MeV})^3(A/100)^{2/3} \quad (12)$$

for E_γ in MeV.

From an analysis of ground-state neutron-capture γ -

ray studies, Bartholomew¹⁶ obtained a value for the constant C of 2.2×10^{-5} . Also, Carpenter¹⁷ obtained a value of 2.7×10^{-5} from resonance neutron-capture γ -ray studies. With Bartholomew's value for C , the single-particle model predicts a value for $\langle \Gamma_{\gamma 0}/D \rangle$ of 6.5×10^{-5} . Therefore, both predictions are about a factor of 2 higher than the value obtained in this experiment.

VI. CONCLUSIONS

The results of this work can be summarized as follows:

1. The cross section is characterized by two very strong lines with many smaller, only partially resolved resonances spread rather uniformly across the range of the measurement.

2. By measurements at a second electron energy, it has been shown that the two strong lines definitely are associated with neutron emission to the ground state of Fe^{55} .

3. For these two resonances the energy resolution was adequate to obtain values for the neutron widths by shape analysis.

4. These resonances almost surely are associated with s -wave neutron emission.

5. The multipolarity of the photon interaction here almost surely is electric dipole. Therefore, the spin of these resonances is 1^- .

6. The γ -ray strength function has been obtained by using the area under the cross-section curve over the full energy range of the measurement. Corrections for contributions from isotopes other than Fe^{56} can reduce this quantity only by about 10%. The effect of magnetic-dipole photon absorption and p -wave neutron emission to the ground state of Fe^{55} cannot be eliminated; any correction for this interaction would reduce further the value of the strength function.

7. Both single-particle and giant-resonance-wing predictions for the strength function are a factor of 2 larger than the value obtained in these experiments.

It should be emphasized that in determining the strength function from the type of experiment outlined here, only the integral of the cross section need be used. Thus, such a measurement of the γ -ray strength functions does not require an energy resolution sufficient to resolve the resonances. The only requirement necessary is that the conditions of the experiment eliminate, with a fairly high degree of certainty, any photon interaction other than electric dipole. If necessary, this can be accomplished by studying the angular distribution of the neutrons. A consideration of isotopes across the periodic table indicates that there are a number of such favorable targets which should allow a systematic in-

¹⁴ P. Axel, Phys. Rev. **126**, 671 (1962).

¹⁵ S. C. Fultz, R. L. Bramblett, J. T. Caldwell, N. E. Hansen, and C. P. Jupiter, Phys. Rev. **128**, 2345 (1962).

¹⁶ G. A. Bartholomew, Ann. Rev. Nucl. Sci. **11**, 259 (1961).

¹⁷ R. T. Carpenter, Argonne National Laboratory Report No. ANL-6589, 1962 (unpublished).

vestigation of the γ -ray strength function as a function of A . Therefore, it should be possible, in a series of experiments such as this, to differentiate between the $A^{2/3}$ and $A^{8/3}$ dependence of $\langle \Gamma_{\gamma_0}/D \rangle$ predicted by the single-particle and giant-resonance models, respectively.

The data-taking rates for this experiment can be improved by a factor of at least 1000 with the best equipment available with existing technology.¹⁸ It is therefore reasonable to expect this technique to become a fruitful source of information for many other properties of nuclei other than those investigated here.

¹⁸ L. M. Bollinger, in Proceedings of the Conference on Cross Section Technology, Washington, D. C., Conf. No. 660303, pp. 1064, 1966 (unpublished).

ACKNOWLEDGMENTS

We should like to acknowledge helpful discussions with Dr. S. C. Fultz and Dr. W. C. Dickinson, and to thank Dr. E. Goldberg for his encouragement. We also wish to thank Capt. R. L. Van Hemert for assistance in the reduction of the data; E. M. Lent for calculations of the bremsstrahlung energy dependence and intensity; J. Nutter and the mechanical technicians for construction and assembly of the equipment required for this experiment; and E. Dante, Jr. and the accelerator operators for the good performance of the machine under unusual operating conditions. We also are indebted to Dr. R. C. Block of the Rensselaer Polytechnic Institute for sending us his high-resolution neutron-capture cross-section data on Fe⁵⁶ prior to publication.

Threshold Photoneutron Cross Section for Be⁹†‡

B. L. BERMAN, R. L. VAN HEMERT,* AND C. D. BOWMAN

Lawrence Radiation Laboratory, University of California, Livermore, California

(Received 10 July 1967)

The Be⁹ (γ, n) Be⁸ cross section was measured as a function of photon energy from less than 1 to about 40 keV threshold, by the threshold photoneutron technique. The cross section rises sharply to a maximum of 1.6 mb at 6 keV above threshold and then decreases slowly to 1.2 mb at 40 keV. An attempt was made to fit these data, and earlier data obtained from monoenergetic γ -ray source measurements, with a curve of the Breit-Wigner form in order to examine the possibility that the shape of the cross section is influenced primarily by a single level near threshold. The results show that such a curve is inadequate to explain the data, and thus indicate that a more complex theory and even better data are needed to understand fully the nature of the cross section near threshold for the Be⁹(γ, n) reaction.

I. INTRODUCTION

THE nature of the photoneutron cross section for the Be⁹ nucleus just above threshold has been a subject of widespread interest, owing to several circumstances. First, the (γ, n) threshold at 1.665 MeV¹⁻⁴ is the lowest for all the stable nuclei, which means that the last neutron in the nucleus is very weakly bound, and hence can be treated as a valence nucleon which sees a nuclear potential attributable to a Be⁸ core. Further, this core breaks up spontaneously into two α

particles, so that it is possible to describe the Be⁹ nucleus as a two- or three-body structure of strongly interacting particles. The photoneutron cross section then can be treated theoretically in a relatively simple way, and is a sensitive function of the nuclear forces employed in such a treatment. Finally, there is a peak in this cross section just above threshold, which is held generally¹ to be ascribable to a state in the excited Be⁹ nucleus which has angular momentum and parity $J^\pi = \frac{1}{2}^+$; thus it should be excited strongly by an electric dipole transition from the $\frac{3}{2}^-$ ground state of Be⁹, and then should decay by s -wave neutron emission to the 0⁺ ground state of Be⁸. The object of the experimental study reported here is the detailed description of the shape of this cross section near threshold.

The Be⁹(γ, n)Be⁸ cross section has been measured in the past in two ways. Standard bremsstrahlung techniques have been used by Walter *et al.*⁵ and by Jakobson,⁶ and both experiments show a peak in the (γ, n) cross section within 50 keV of the threshold of

† This work was performed under the auspices of the U. S. Atomic Energy Commission.

‡ A preliminary account of this work appeared as B. L. Berman, R. L. Van Hemert, and C. D. Bowman, *Bull. Am. Phys. Soc.* **12**, 483 (1967).

* Major, United States Air Force. The views expressed herein are those of the author and do not necessarily reflect the views of the United States Air Force or the Department of Defense.

¹ T. Lauritsen and F. Ajzenberg-Selove, *Nucl. Phys.* **78**, 1 (1966) and references therein.

² D. R. Connors and W. C. Miller, *Bull. Am. Phys. Soc.* **1**, 340 (1956).

³ R. C. Mobley and R. A. Laubenstein, *Phys. Rev.* **80**, 309 (1950).

⁴ J. H. E. Mattauch, W. Thiele, and A. H. Wapstra, *Nucl. Phys.* **67**, 32 (1965).

⁵ R. L. Walter, M. F. Shea, and W. C. Miller, *Bull. Am. Phys. Soc.* **5**, 229 (1960).

⁶ M. J. Jakobson, *Phys. Rev.* **123**, 229 (1961).